Novel Antenna-Integrated Photodiodes With Strained Absorbers Designed for Use as Terahertz Sources

Ian D. Henning, Michael J. Adams, Martin Vaughan, Thomas Abraham, Yun Sun, Angela Dyson, David G. Moodie, Dave C. Rogers, Paul J. Cannard, Sukhjiban Dosanjh, Mark Skuse, and Richard J. Firth

***Abstract*—We present experimental results on the performance of antenna-integrated photodiodes intended for use as photomixers to provide a tunable broadband source of terahertz (THz) radiation. In a balanced strain-absorber structure, we show that the introduction of strain has proved effective in enhancing the performance at frequencies above 500 GHz. A comparison of strained and unstrained devices confirms this claim. These structures are integrated with a range of antennas, including log periodic and slot–horn types, designed for wideband THz emission. Using the devices as photomixers for the outputs from a DFB laser and an external cavity laser in the 1550 nm telecom window, tunable emission is demonstrated over the range from 100 GHz to 1.8 THz.**

***Index Terms*—Photodetectors, planar antenna, strain, submillimeter-wave generation.**

I. Introduction

RECENT years have seen considerable research interest in novel means of generating and detecting terahertz (THz) radiation using optoelectronic devices (for a review, see [1]). One promising approach that has attracted much attention is based on the quantum cascade laser (QCL), which offers the prospect of a compact electrically pumped continuous source of radiation in the range 1–5 THz. However, while QCL lasers have demonstrated relatively high output powers [1], the problem of operation at room temperature remains unsolved; a review of this aspect is given in [2], where it is noted that the optimum QCL emission frequency for high-temperature operation appears to be around 3 THz. Currently, operation at 186 K for 3.9 THz emission [3] based on a diagonal design is the highest temperature yet achieved, although the use of a strong magnetic field has pushed the operating temperature to 225 K for emission at 3 THz [4]. Another contender for a compact solid-state source of THz radiation is the approach of photomixing of optical signals from two room-temperature semiconductor lasers emitting near the telecom wavelength of 1550 nm. Photomixers that have been used include conventional photodiodes [5] and photoconductors [6], but the most promising approach to date is based on the unitravelling-carrier (UTC) photodiode [7]. The latter has been used to generate an output power up to 25 μW at 0.9 THz [8], which represents the highest power generated by a photomixer source at this frequency to date.

Recent research has focused on optimization of the UTC device structure and doping with the objective of increased frequency response and enhanced output saturation [9]–[13]. In our previous work [11], we found that enhanced performance could be obtained by using reduced doping in the absorber of a conventional UTC, leading to a structure where both electrons and holes contribute to the photocurrent termed a "composite p-i-n" (CPIN). A schematic band diagram for a CPIN is shown in Fig. 1. We also found that type-II conduction band line up with materials based on GaAsSb-InP [14] led to improved performance, although the low electron mobility in lattice-matched Sb materials restricted the improvement to thin absorbers only (<50 nm). However, experimental work has shown this material system to be challenging in terms of growth and fabrication. We thus propose an alternative approach for enhancing performance by incorporating lattice strain in the absorber of an InGaAs/InP CPIN photodiode. Strain has been widely used in optimizing the performance of various devices, particularly in conjunction with quantum-confined structures (see e.g., [15]). While strain has been used to enhance the spectral response of photodetectors [16], we are not aware of reported use to enhance their high-frequency performance, where the introduction of strain offers some additional device engineering advantages, which are as follows.

1) Strain between layers leads to a variation in band lineup, offering the prospect of reducing the conduction band step between an InGaAs absorber and the collector, thus leading to pseudo-type-II behavior.
2) Tensile strain leads to light-hole–heavy-hole splitting in the valence band, and for a CPIN where both electrons and holes contribute to performance, this offers the prospect of enhanced hole mobility and transport in the depleted p-type part of the absorber.
3) Tensile strain leads to bandgap reduction and compressive strain leads to increased bandgap, thus offering the

Manuscript received February 4, 2010; revised March 17, 2010; accepted April 14, 2010. Date of publication June 21, 2010; date of current version February 4, 2011. This work was supported by the U.K. Engineering and Physical Sciences Research Council under the Portable Terahertz Systems based on Advanced InP Technology (PORTRAIT) Grant Reference EP/D502225/1.

I. D. Henning, M. J. Adams, T. Abraham, and Y. Sun are with the School of Computer Science and Electronic Engineering, University of Essex, Colchester, Essex, CO4 3SQ, U.K. (e-mail: idhenn@essex.ac.uk; adamm@essex.ac.uk; tjabra@essex.ac.uk; ysunf@essex.ac.uk).

M. Vaughan was with University of Essex, Colchester, Essex, CO4 3SQ, U.K. He is now with the Tyndall Institute, Cork, Ireland (e-mail: martin.vaughan@tyndall.ie).

A. Dyson was with University of Essex, Colchester, Essex, CO4 3SQ, U.K. She is now with the Department of Physics, University of Hull, Hull, HU6 7RX, U.K. (e-mail A.Dyson@hull.ac.uk).

D. G. Moodie, D. C. Rogers, P. J. Cannard, S. Dosanjh, M. Skuse, and R. J. Firth are with CIP Technologies, Martlesham Heath, Ipswich, IP5 3RE, U.K. (e-mail: dave.moodie@ciphotonics.com; dave.rogers@ciphotonics.com; paul.cannard@ciphotonics.com; jeevan.dosanjh@ciphotonics.com; mark.skuse@ciphotonics.com; rick.firth@ciphotonics.com).

Color versions of one or more of the figures in this paper are available online at http://ieeexplore.ieee.org.

Digital Object Identifier 10.1109/JSTQE.2010.2049196

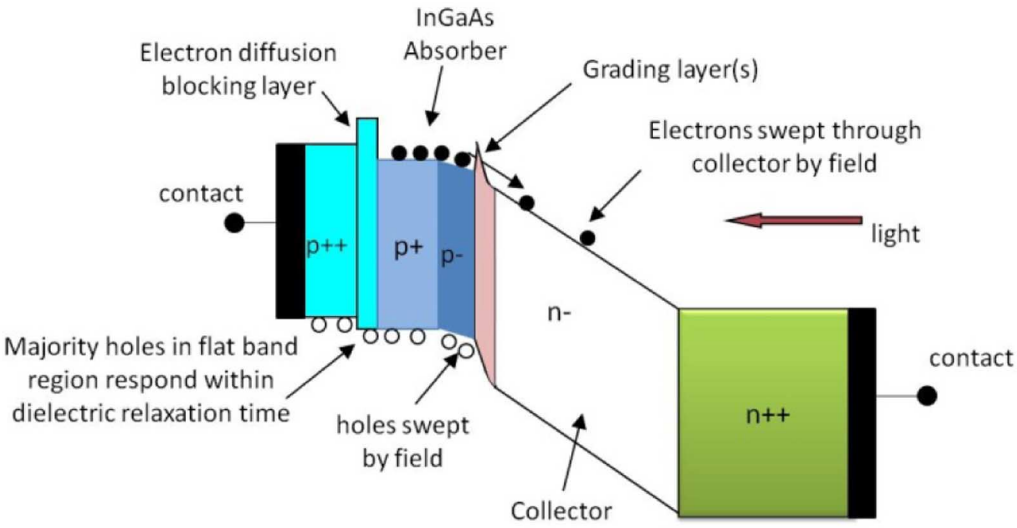

Fig. 1. Schematic band diagram of a CPIN.

prospect of tailoring the bandedge across an absorber to enhance carrier transport.

With reference to the device schematic in Fig. 1, we seek to gain best advantage from these effects by forming a balanced strain absorber; near the grading layers and where the p-layer is depleted, we grow a tensile strained region, near the electron diffusion blocking layer, we grow a compressive strained region, while overall, the strain is balanced across the structure. Such an approach offers the prospect of near type-II behavior with a high-mobility InGaAs material system, graded bandgap across the absorber, and enhanced electron confinement in the absorber. We investigated the efficacy of this approach in two different device-antenna structures, as described in Section II. In Section III, the experimental setup is described, while results for the two structures are given in Section IV. We previously published some initial device results [17], but here, we present the novel use of strain with new and more detailed results.

II. Device Description

Initially, two epitaxial device wafers were grown by CIP on semi-insulating (SI) InP substrates using metallorganic vapor-phase epitaxy (MOVPE). With reference to the schematic in Fig. 1, both samples had a 75-nm-thick InGaAs absorber layer. However, in one wafer, the absorber layer was unstrained, while in the other, the InGaAs was strained with a linear gradation from a compressive strain at the top of the absorber layer to a tensile strain at the bottom of the absorber layer (this difference was confirmed post growth by X-ray rocking curve analysis). In both cases, quaternary InGaAsP p- and n-contact layers were employed with the latter also functioning as a passive optical input waveguiding layer, which evanescently coupled light to the detector. The strained wafer (designated AX1652) employed a 145-nm-thick n-InP collector layer beneath the absorber layer with 20 nm of n-InGaAsP intermediate lattice-matched quaternary transition layers (doped $5 \times 10^{16} - 2 \times 10^{17}\ \mathrm{cm}^{-3}$) in between the collector and absorber bringing the total intended depletion thickness to 190 nm. In the unstrained wafer (grown in a different MOVPE growth machine and designated MW1278), the n-InP collector layer was 5 nm thicker and the n-InGaAsP transition layers in between the collector and absorber were 12 nm thicker than in the strained wafer. In each case, the collector was intentionally doped at $\sim 5 \times 10^{16}\ \mathrm{cm}^{-3}$, and overall, the doping levels of the n-type grading and collector layers in the two wafers were chosen such that the device would be fully depleted at zero-applied bias. In both cases, the top p+ 50 nm of the absorber layer was intentionally doped at $\geq 1 \times 10^{18}\ \mathrm{cm}^{-3}$. However, in the unstrained wafer (MW1278), the bottom p− 25 nm was not intentionally doped. Since Zn will diffuse during the wafer growth process, this latter region will end up lowly p-doped (estimated to be in the range $3 \times 10^{16} - 5 \times 10^{16}\ \mathrm{cm}^{-3}$), the extent of the diffusion being limited by the n-type grading layers. In the strained wafer (AX1652), the bottom p− 25 nm was doped at $5 \times 10^{17}\ \mathrm{cm}^{-3}$. With both of these structures, the absorber doping is designed for device operation where both holes and electrons contribute to the photocurrent (a CPIN, as reported in [11]). This contrasts with a conventional UTC (see e.g., [7]), where the absorber is uniform and highly p-doped and only one carrier type, typically electrons, contributes to the photocurrent. Another difference was that the doping level in the n-contact/buffer layers was higher in the strained wafer. The strain in wafer AX1652 intentionally grades linearly from 1% tensile strain near the collector to 1% compressive stain near the p-contact layer (whereas MW1278 is lattice matched throughout). These values (which were confirmed by post growth X-ray rocking curve analysis) were selected as a starting point based on related published work [16], [18]: a high value of strain would potentially introduce large changes in bandgap, light-hole/heavy-hole splitting, and band offsets, while too much strain, particularly approaching the critical thickness, could lead to a reduction in material quality making fabrication difficult and obviating any advantageous effects. The value chosen seemed to offer a compromise: 1% tensile offering 50 mV reduction of conduction band offset and 50 mV light-hole/heavy-hole splitting,

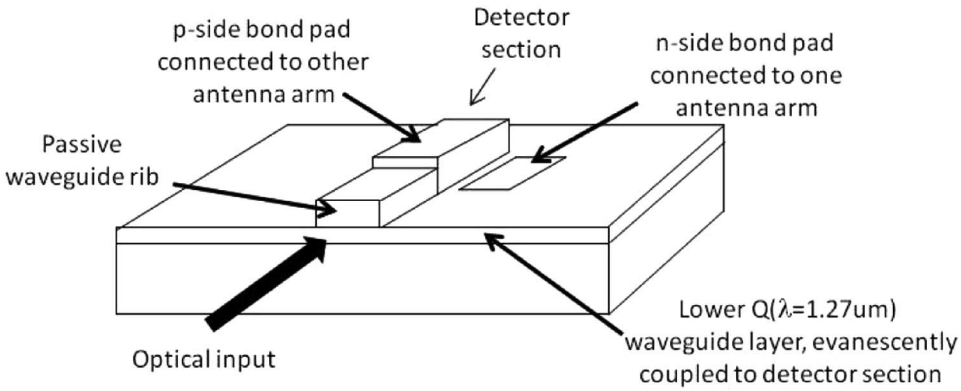

Fig. 2. Schematic of integrated detector-waveguide antenna.

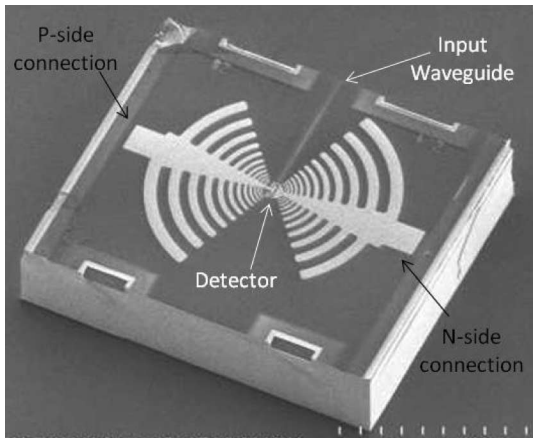

Fig. 3. SEM of integrated waveguide-detector LPA.

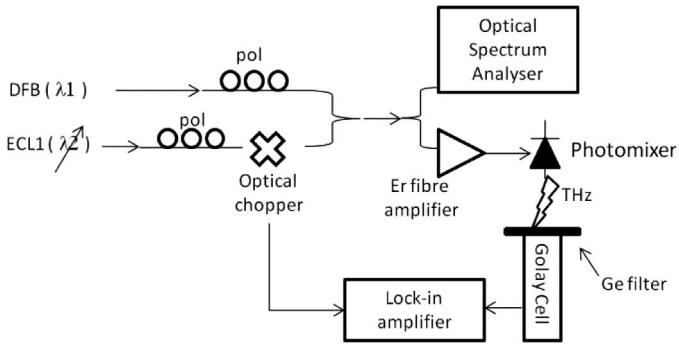

Fig. 4. Diagram of the THz measurement setup.

and 1% compressive strain offering 40 mV increase in bandgap (all values arranged to be greater than the thermal energy at room temperature).

The schematic diagram of the final device structure shown in Fig. 2 depicts a simple (3 μm wide) rib-loaded passive waveguide section into which light is edge-coupled from a lens-ended fiber. Light propagates along this guide and evanescently couples into a short (3 μm wide and 15 μm long) detector section. The two wafers were fabricated using the same mask set, which included antenna variants, one of which was a log-periodic antenna (LPA) designed to cover the band 0.1–1 THz (see Fig. 3). This had a radius of 200 μm and 12 "teeth." The antennas that were formed on top of a 2-μm-thick silicon oxynitride dielectric layer, which was deposited on the InP substrate, were simulated using both CST-Microstripes^{TM} and the Momentum part of Agilent ADS^{TM} simulation tools. When completed, the integrated antenna CPINs were thinned, diced, and mounted within a metal package on top of a high-resistivity silicon carrier wafer. A hole was provided in the metal package to allow the THz emission to exit through the InP substrate/Si carrier.

III. Experimental

A schematic diagram of the experimental setup for measuring the THz emission is shown in Fig. 4. Polarization-controlled light from a finely tunable (2 nm) DFB laser emitting at 1539 nm and a widely tunable (1510–1590 nm) external cavity laser (ECL) were combined using a fiber coupler. The resulting signal was amplified using a high-saturation power (adjustable to +20 dBm) Erbium-doped fiber amplifier (EDFA). This high-power optical signal was launched into the antenna-integrated CPIN THz photomixer. A monitor signal was tapped off and an accurate determination of the difference frequency was made using an Ando optical spectrum analyzer. To reduce the influence on the measurements of spontaneous–spontaneous beat noise from the EDFA, the output from the DFB laser was fed directly through holding it in saturation. The output from the ECL was then optically chopped and combined with the DFB. The THz emission was measured using a calibrated Microtech Golay cell with a PTFE window. The output from the Golay was fed into a lock-in amplifier with a reference provided by the optical chopper. Experience showed that scattered 1500-nm radiation leaking through the substrate was significant, and therefore, a calibrated Grubb and Parsons 640-μm-thick Ge multilayer infrared filter was used to remove this. To enhance the collection of THz emission through the substrate, a high-resistivity Si lens was chosen by taking account of the thickness of the SI InP substrate and high-resistivity Si carrier wafer(s). Frequency-response measurements were made by utilizing the (tunable) different frequency of the lasers to generate a beat signal in the photodiode and by measuring the resulting THz emission with the Golay cell.

IV. Results and Discussion

A. Results on Integrated-Waveguide-Antenna CPINs

The device *I/V* characteristics showed consistent differences in reverse leakage current between wafers. By comparing these, we observed that on average the leakage current in devices fabricated on the strained wafer were up to ten times higher than those found when using the unstrained wafer (e.g., 280 nA, cf., 2860 nA at -3 V). While this may cause problems for photodetectors used in high-sensitivity applications, i.e., optical receivers, it is not thought to be an issue for devices used as photomixers in THz applications, where photocurrents of tens of milliampere might be anticipated. From device characteristics, the series resistances of the unstrained devices were estimated to be in the range 20–30 Ω, while those for the strained devices were less than 15 Ω. The capacitance of the integrated devices was measured as a function of device length for the different antenna structures that were included on the wafer. From this, it was deduced that 15-μm-long absorber sections from both wafers had a capacitance of 30 fF, which is close to the theoretically calculated value of 27 fF. This confirms the similarity of the doping profile/layer thicknesses in both wafers.

Fig. 5 (a)–(d) shows plots of the characteristics of two devices made from the two wafers. In Fig. 5(b) and (d), we also show both the dc photocurrent and emitted THz power at 300 GHz as a function of input optical power. The measurements are taken at room temperature with the device on a heat sink, but without temperature control. It is noticeable that the strained CPIN structure exhibits far more favorable saturation behavior than the nonstrained device particularly at low reverse bias (in fact even at zero bias, the responsivity was maintained up to 40 mW optical input power, and THz emission continued to increase up to 14 mW input optical power, and 4 mA average photocurrent). In contrast, the unstrained device shows more pronounced saturation characteristics and the THz emission was a stronger function of reverse bias [see Fig. 5(d)]. While this difference in behavior may be in part due to the higher series resistance on the unstrained devices, it may also be indicative of improved transport as carrier pileup, particularly at interfaces within such structures, alters the internal electric fields and hence strongly influences the saturation characteristics [11].

Fig. 6 shows a plot of the measured THz emission as a function of frequency for both devices. Since both were made using the same mask set and fabrication procedure, their responses should be comparable. Given a device capacitance of $\sim$30 fF and a nominal total series impedance of around 60–70 Ω, we estimate a -3 dB electrical bandwidth of $<$100 GHz for both devices. Based on the modeling in [11], we anticipate this to be well below the intrinsic bandwidth of the devices, which we would expect to be in the range 200–300 GHz. Thus, in terms of overall characteristic, we anticipate both devices to show a capacitance-limited response, which initially rolls off at 6 dB per octave above this frequency ($\sim$100 GHz, which is the lower limit of the antenna). We might also anticipate seeing a second pole appearing with a faster rate response roll off above the intrinsic device bandwidth in the range 200–300 GHz.

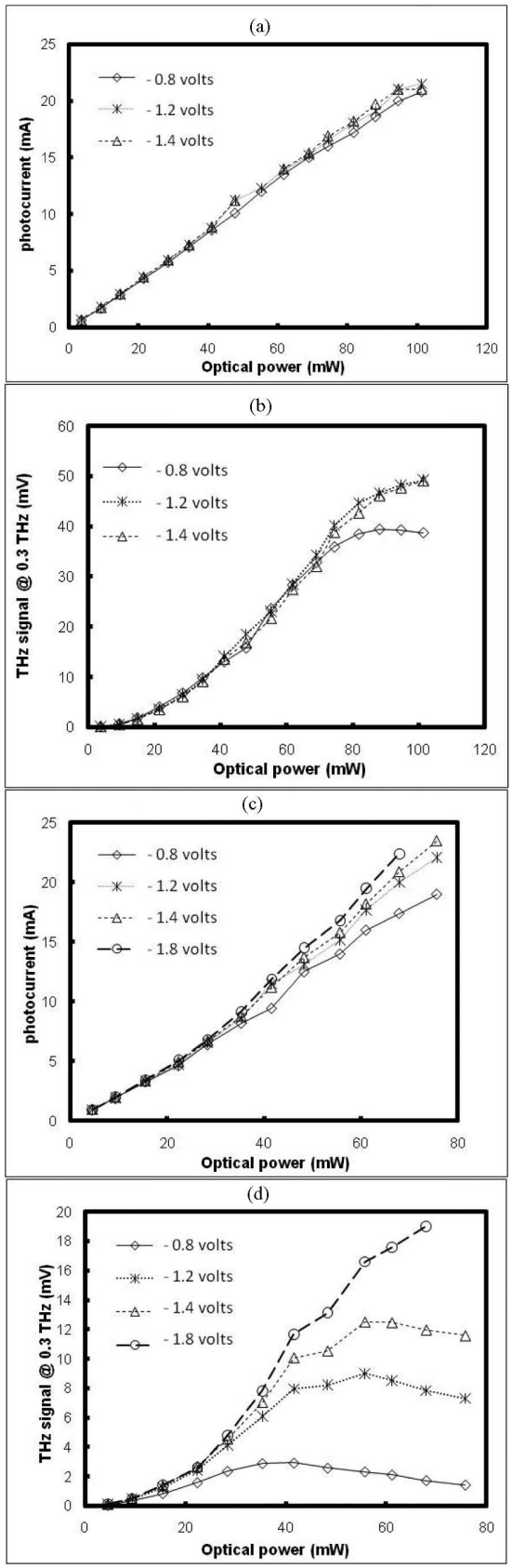

Fig. 5. Photocurrent versus input optical power measured at different reverse-bias voltages (as indicated) for (a) strained device and (c) unstrained device. THz emission (Golay signal in millivolts) measured at 300 GHz versus input optical power for (b) strained device and (d) unstrained device.

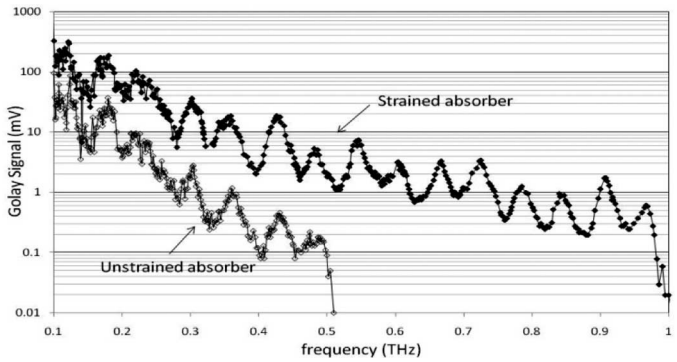

Fig. 6. THz emission measured using the Golay cell as a function of beat frequency at ∼14 mA photocurrent and −1 V reverse bias; #03814 strained device, #03813 unstrained device

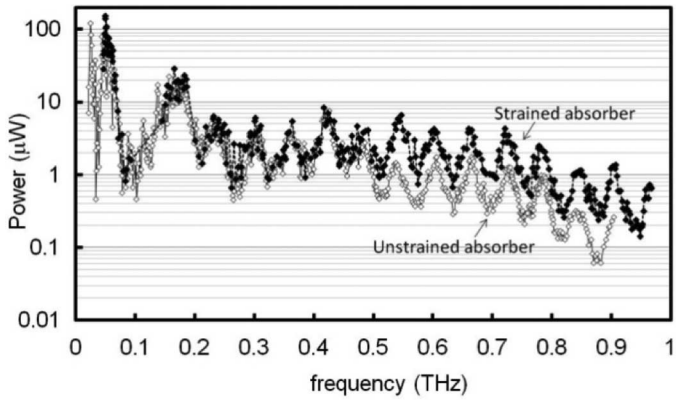

Fig. 7. Frequency response of integrated slot–horn antenna stub-CPIN devices showing influence of strain. (Filled diamonds) Strained device, 5.6 mA photocurrent and (open diamonds) unstrained device, 5.3 mA photocurrent, both reverse biased at −1 V.

Both devices were operated under the same conditions, reverse biased at −1 V and illuminated to produce ∼14 mA of photocurrent. From the results in Fig. 6, it is clear that both devices do, indeed, exhibit a falling response above 100 GHz (the lower limit of the LPA antenna). However, under these conditions, the introduction of strain into the absorber layer has resulted in a useful increase in THz output power at higher frequencies and an increase in ultimate bandwidth. Furthermore, it appears to have been effective in reducing the final rate of roll off with frequency. The difference in emitted THz power has increased by a factor of over 2–3 at 150 GHz, to over 10 above 500 GHz. Given that the measurements are ultimately limited by noise, THz emission can be seen up to about ∼500 GHz for the nonstrained device, but with strain, a response to 1.1 THz is observable (it should be noted that the periodic structure seen on these plots occurs in all of our measurements and we believe this arises mainly from the Ge filter, but in the case of the LPA also includes a contribution from the antenna characteristics).

B. Results on Antenna-Integrated Stub-CPINs

To further test the validity of these observations and to eliminate as far as possible any extrinsic effects (i.e. series resistance, slight difference in grading layer thickness, absorber doping profile, and growth kit dependence), two further new wafers were grown and fabricated into devices. This time both wafers were grown in the same MOVPE machine to eliminate any growth-kit-dependent effects. The wafers were intentionally identical in layer composition and doping profile (both with the absorber doping the same as that used in AX1652), but with once again, one of the wafers having a linearly graded strained absorber and the other being lattice-matched throughout. However, this time the thickness of the InP-collector region of both wafers was increased from 0.15 to 0.26 μm, and a different antenna-integrated device structure was used (an edge-coupled detector, termed a stub-CPIN, integrated with a slot–horn antenna to be reported elsewhere). This approach was hoped to show if strain-induced performance gains could still be observed in completely different device and antenna structures, thus eliminating effects arising from antenna/physical device design. On

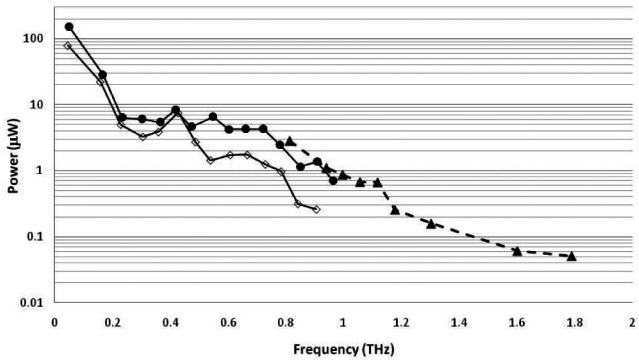

Fig. 8. Comparative frequency response for slot–horn antenna-integrated stub-CPINs for both strained and unstrained absorbers. (Open diamonds) Unstrained device and (closed circles and triangles) strained devices.

average and in common with previous results, the leakage currents at −3 V were slightly higher (approximately four times) for the strained wafers than for the nonstrained wafers, namely 160 nA, cf., 40 nA, although this was again stable and did not appear to increase over the period of the measurements. Capacitance of the two sets of devices with 12.5-μm-long absorber sections (3 μm wide) was very similar at 19 fF, as was responsivity at 0.3–0.35 A/W (an improvement obtained with this new edge-placed design). The frequency response results obtained on two typical devices are plotted in Fig. 7 for wafers AX1666 A (lattice-matched absorber) and AX1665 A (strained absorber).

To more fully illustrate the differences between these, we show a further plot in Fig. 8 taken under the same conditions, but tracing just the peaks in the periodic structure of Fig. 7 and extending the plot to higher frequencies.

Once again, the devices made from wafers with strained-absorber regions show enhanced performance at high frequency (above 500GHz), although the differences are not as significant as those shown in Fig. 6. The overall frequency response of these photodiodes involves a combination of factors, one of which is the carrier transit time across the drift region. The thickness of the drift region for the devices in Fig. 6 is 0.15 μm, whereas for

those in Fig. 8, it is 0.26 μm. Since the overall bandwidth arises from a combination of a number of time constants [12], to a first approximation, while still seeing benefits from the use of strain, we might anticipate that the longer drift time for the second set of devices might reduce somewhat the benefits accrued at higher frequency. We believe this to be in accord with the experimental results.

In the introduction, we discussed three possible mechanisms by which strain might yield favorable performance improvements: conduction band offset reduction at the absorber grading layer interface, reduced hole-effective mass in the depleted p-doped part of the absorber, and bandgap grading across the absorber. In addition an increase in conduction band offset between the absorber and the p-doped electron-diffusion blocking layer might also be expected, although with the range of structures modeled in the work reported in [11], we did not see a strong dependency of device bandwidth on electron leakage into the p+ cap/contact layers. However, the earlier modeling [11] did suggest two approaches that offered enhanced high-frequency performance (slower roll off). The first of these was reduced absorber doping, and the simulated change in device frequency response as the absorber doping level is reduced [11, Fig. 9]. Thus, we believe that the responses we have measured can be attributed in part to the absorber doping profile chosen. The second approach, which offered favorable performance, was the use of type-II conduction band lineup, i.e., reduced conduction band offset. This was modeled in [11] for InGaSb/InP photodiodes, but the benefit was only seen with thin (<50 nm) absorber layers due to the low electron mobility in InGaSb. Moreover, such thin absorber layers pose design challenges, since even for edge-coupled devices with additional wave guiding layers, it is difficult to achieve high optical confinement, and hence, good responsivity without resorting to long structures with accompanying increase in area and device capacitance. Since the results we report here were obtained using an InGaAs absorber that has high electron mobility, we might similarly expect bandwidth improvements for any additional strain-induced reduction in conduction band offsets (moving toward type-II behavior), but given the higher InGaAs electron mobility, this might now occur in thicker absorbers. This would allow for easier engineering of short, high-responsivity, low-capacitance devices. Furthermore, we have yet to model the effect of strain-induced bandgap grading and reduced hole effective mass, while we anticipate both these effects to play some part in device performance, we have yet to identify their relative contributions. In addition, we have investigated only one "recipe," and it is feasible that further optimization is possible both through doping and the selection of the amount of strain and its distribution. For example, for type-II-like behavior, it may be best to incorporate strain across the absorber and grading layer interfaces to remove any conduction band spikes only. Moreover, while we have investigated the use of strain in junction photodiodes, it may also be the case that strain-induced effects could also be used to advantage in photoconductive devices. We anticipate further work in this area both in terms of modeling, experimental wafer growth, and device fabrication to investigate fully the potential performance gains that might be achieved.

V. Conclusion

In this paper, we present experimental results on antenna-integrated CPIN photodiodes. We show promising increase in high-frequency performance and saturation characteristics through the use of strain in a balanced strain-absorber structure. Comparisons of strained and unstrained devices confirm this performance enhancement. In the detector and antenna designs investigated, we have shown that this has proved effective in enhancing the high-frequency performance (>500 GHz) for CPINs designed as photomixers for THz sources. Further work on edge-coupled stub-CPIN photomixers will be reported in a subsequent paper.

Acknowledgment

The authors would like to thank Prof. E. Linfield and his group at the University of Leeds for help in characterization of various THz components, and A. Boland-Toms and J. Rowlands at the University of Essex for technical support.

References

[1] D. Saeedkia and S. Safavi-Naeini, "Terahertz photonics: Optoelectronic techniques for generation and detection of terahertz waves," *J. Lightw. Technol.*, vol. 26, no. 15, pp. 2409–2423, Aug. 2008.

[2] M. A. Belkin, Q. J. Wang, C. Pflugl, A. Belyanin, S. P. Khanna, A. G. Davies, E. H. Linfield, and F. Capasso, "High-temperature operation of terahertz quantum cascade laser sources," *IEEE J. Sel. Topics Quantum Electron.*, vol. 15, no. 3, pp. 952–967, May/Jun. 2009.

[3] S. Kumar, Q. Hu, and J. L. Reno, "186 K operation of terahertz quantum-cascade lasers based on a diagonal design," *Appl. Phys. Lett.*, vol. 94, pp. 131105-1–131105-3, 2009.

[4] A. Wade, G. Fedorov, D. Smirnov, S. Kumar, B. S. Williams, Q. Hu, and J. L. Reno, "Magnetic-field-assisted terahertz quantum cascade laser operating up to 225 K," *Nat. Photon.*, vol. 3, no. 1, pp. 41–45, Jan. 2009.

[5] P. G. Huggard, B. N. Ellison, P. Shen, N. J. Gomes, P. A. Davies, W. Shillue, A. Vaccari, and J. M. Payne, "Generation of millimetre and sub-millimetre waves by photomixing in 1.55 μm wavelength photodiode," *Electron. Lett.*, vol. 38, no. 7, pp. 327–328, Mar. 2002.

[6] J. Mangeney, A. Merigault, N. Zerounian, P. Crozat, K. Blary, and J. F. Lampin, "Continuous wave terahertz generation up to 2 THz by photomixing on ion-irradiated $In_{0.53}Ga_{0.47}As$ at 1.55 μm wavelengths," *Appl. Phys. Lett.*, vol. 91, no. 24, pp. 241102-1–241102-2, Dec. 2007.

[7] H. Ito, S. Kodama, Y. Muramoto, T. Furuta, T. Nagasuma, and T. Ishibashi, "High-speed and high-output InP-InGaAs unitravelingcarrier photodiodes," *IEEE J. Sel. Topics Quantum Electron.*, vol. 10, no. 4, pp. 709–727, Jul./Aug. 2004.

[8] C. C. Renaud, M. Robertson, D. Rogers, R. Firth, P. J. Cannard, R. Moore, and A. J. Seeds, "A high responsivity, broadband waveguide uni-travelling carrier photodiode," in *Proc. SPIE*, vol. 6194, 2006, p. 61940C.

[9] P. D. Yoder and E. J. Flynn, "Quasi-unipolar InGaAs/InP photodetection for enhanced optical saturation power and maximal bandwidth," *Appl. Phys. Lett.*, vol. 91, no. 6, pp. 062114-1–062114-3, Aug. 2007.

[10] J. Klamkin, Y.-C. Chang, A. Ramaswamy, L. A. Johansson, J. E. Bowers, S. P. DenBaars, and L. A. Coldren, "Output saturation and linearity of waveguide unitraveling-carrier photodiodes," *IEEE J. Quantum Electron.*, vol. 44, no. 4, pp. 354–359, Mar./Apr. 2008.

[11] A. Dyson, I. D. Henning, and M. J. Adams, "Comparison of type-I and type-II heterojunction unitraveling-carrier photodiodes for terahertz generation," *IEEE J. Sel. Topics Quantum Electron.*, vol. 14, no. 2, pp. 277–283, Mar./Apr. 2008.

[12] B. Banik, J. Vukusic, H. Hjelmgren, and J. Stake, "Optimization of the UTC-PD epitaxy for photomixing at 340 GHz," *Int. J. Infrared Milli. Waves*, vol. 29, no. 10, pp. 914–923, Oct. 2008.

[13] Y.-T. Li, J.-W. Shi, C.-Y. Huang, N.-W. Chen, S.-H. Chen, J.-I. Chyi, Y.-C. Wang, C. -Sh. Yang, and C.-L. Pan, "Characterization and comparison of GaAs/AlGaAs uni-traveling carrier and separated-transport-recombination photodiode based high-power sub-THz photonic transmitters," *IEEE J. Quantum Electron.*, vol. 46, no. 1, pp. 19–27, Jan. 2010.

[14] L. G. Zheng, X. Zhang, Y. P. Zeng, S. R. Tatavarti, S. P. Watkins, C. R. Bolognesi, S. Demiguel, and J. C. Campbell, "Demonstration of high-speed staggered lineup GaAsSb-InP unitravelling carrier photodiodes," *IEEE Photon. Technol. Lett.*, vol. 17, no. 3, pp. 651–653, Mar. 2005.
[15] J. J. Coleman, "Strained-layer InGaAs quantum-well heterostructure lasers," *IEEE J. Sel. Topics Quantum Electron.*, vol. 6, no. 6, pp. 1008–1013, Nov./Dec. 2000.
[16] J. Kaniewski and J. Piotrowski, "InGaAs infrared detectors," *Opto-Electron. Rev.*, vol. 5, no. 3, pp. 225–231, 1997.
[17] I. D. Henning, Y. Sun, M. P. Vaughan, A. Dyson, T. Abraham, M. J. Adams, D. G. Moodie, D. C. Rogers, S. Dosanjh, and R. Firth, "Widely tunable optoelectronic source of continuous-wave terahertz radiation," *Electron. Lett.*, vol. 45, no. 24, pp. 1252–1253, Nov. 2009.
[18] T. J. C. Hosea and G. Rowland, "Photomodulated reflectance of tensilely strained InGaAs/InGaAsP quantum well structures," *Semicond. Sci. Technol.*, vol. 13, no. 2, pp. 207–213, Feb. 1998.

Ian D. Henning received the B.Sc. degree (first class honors) in applied physics and the Ph.D. degree from the University of Wales, Cardiff, U.K., in 1976 and 1979, respectively.

In 1980, he was in the Devices Division, British Telecom Research Laboratories, Martlesham Heath, U.K., where he was engaged in research specializing in theory and measurements of semiconductor lasers. In 2002, he joined as a Professor in the Department of Electrical Systems Engineering, School of Computer Science and Electronic Engineering, University of Essex, Colchester, U.K. He is the author or coauthor of numerous papers and a coauthor of two books. He holds ten patents. His current research interests include optoelectronic devices and electronic/photonic device integration.

Dr. Henning is a Fellow of the Institute of Physics and Institute Engineering and Technology, a Chartered Physicist, and a Chartered Engineer.

Michael J. Adams received the Ph.D. degree in laser theory from the University of Wales, Cardiff, U.K., in 1970.

Since 1996, he has been a Professor in the School of Computer Science and Electronic Engineering, University of Essex, Colchester, U.K. He was involved in optoelectronics research and development in industries (Plessey, BT) for 15 years and in academia (University of Cardiff, University of Southampton, and University of Essex) for 25 years. He has authored or coauthored in the field of optoelectronics for many years, including a standard text on optical waveguide theory and two books in semiconductor lasers and optical fibers for use in telecommunications. His current research interests include semiconductor lasers, optical amplifiers, optical waveguides, optical bistability, semiconductor nonlinear optics and optical switching devices, and nonlinear dynamics of lasers.

Martin Vaughan received the B.Sc. (Hons.) degree in physics and applied mathematics from the Open University, Milton Keynes, U.K., and the M.Sc. degree in physics of laser communications and the Ph.D. degree from the University of Essex, Colchester, U.K.

He was in the School of Computer Science and Electronic Engineering, University of Essex, where he was engaged in research on the experimental characterization of novel terahertz sources. He is currently in the Photonics Theory Group at the Tyndall National Institute, Cork, Ireland, where he is involved in research on *ab initio* electronic calculations and the transport theory of novel alloys for photonic and complementary metal–oxide–semiconductor applications.

Thomas Abraham received the B.Sc. degree in applied physics from the Warsaw University of Technology, Warsaw, Poland, in 2004, and the M.Phil. degree in electronics engineering from the University of Essex, Colchester, U.K.

He is currently in the School of Computer Science and Electronic Engineering, University of Essex.

Yun Sun received the Ph.D. degree in electronic systems engineering from the University of Essex, Colchester, U.K., in 2009.

She is currently a Research Assistant at the University of Essex. Her research interests include novel semiconductor materials and development of novel optoelectronic devices.

Angela Dyson received the B.Sc. (Hons.) degree in theoretical physics and the Ph.D. degree in theoretical plasma physics from the University of Essex, Colchester, U.K., in 1994 and 1999, respectively.

Since 2007, she has been a Lecturer in the Department of Physics, University of Hull, Hull, U.K. For 11 years, she has worked in the area of semiconductor device theory and modeling. Her current research interests include high field transport, device simulation, and compact sources of terahertz radiation.

David G. Moodie was born in Leicester, U.K., in 1968. He received the B.Sc. degree in physics from the University of Durham, Durham, U.K., in 1989, the M.Sc. degree in telecommunications engineering from the University of London, London, U.K., in 1995, and the Ph.D. degree from Imperial College, London, in 2002.

In 1989, he was at BT Laboratories, U.K., where he was engaged in research on the development of a range of optoelectronic components. From 2000 to 2003, he was a Project Manager at Corning Research Center, U.K. Since 2003, he has been at CIP Technologies, Martlesham Heath, Ipswich, U.K. His current research interests include product management, project management, device design, electroabsorption modulators, photonic integration, photodiodes, and terahertz technologies.

Dave C. Rogers was born in Bromley, U.K., in 1960. He received the B.A. degree in physics and the D.Phil. degree in semiconductor physics from the University of Oxford, Oxford, U.K., in 1982 and 1987, respectively.

In 1986, he was at BT Laboratories, U.K., where he was engaged in research on design, fabrication, and analysis of semiconductor optical devices, special optical fibers, and planar silica waveguides. From 2000 to 2003, he was a Senior Scientist at the Corning Research Center, U.K. Since 2003, he has been with CIP Technologies, Martlesham Heath, Ipswich, U.K. His current research interests include hybrid device design and project management, and all aspects of photonic integration.

Dr. Rogers is a member of the Institute of Physics and a Chartered Physicist.

Paul J. Cannard was born in Somerset, U.K. He received the B.Sc. (Hons.) degree in metallurgy and materials science from University College, Cardiff University, Cardiff, U.K., in 1985, and the Ph.D. degree from the University of Wales, Wales, U.K., in 1988.

In 1988, he was at BT Laboratories, U.K., where he was engaged in research on the surface analysis of a range of materials with special interest in optoelectronic components. From 2000 to 2003, he was the Molecular Beam Epitaxy Scientist at Corning Research Center, U.K. Since 2003, he has been at CIP Technologies, Martlesham Heath, Ipswich, U.K., where he has been involved in working on metal–organic vapor-phase epitaxy. His current research interests include epitaxy development and supply, semiconductor optical amplifiers, electroabsorption modulators, photonic integration, and photodiodes.

Dr Cannard is an Associate Member of the Institute of Materials, Minerals, and Mining.

Sukhjiban Dosanjh received the B.Sc. (Hons.) degree in chemical physics from the University of Kent, Kent, U.K., in 1988, and the Ph.D. degree from Imperial College, London, U.K. on the growth by molecular beam epitaxy (MBE) and optical characterization of highly strained materials, such as InAs on GaAs.

He is currently at CIP Technologies, Martlesham Heath, Ipswich, U.K. He has more than 17 years experience working in the metal–organic vapor-phase epitaxy (MOVPE) and MBE technology areas for CIP Technologies, Agilent Technologies, and previously for BT Labatories. He was a Sales Support Engineer at Oxford Instruments supporting its MBE business. He was a Business Development Manager with RTA Instruments. His research interests include projects with the growth of 1300-nm InP-based lasers and detectors, 1550-nm InP-based lasers, development and application of new precursors for current-blocking layers in optical devices, growth of antimonides, and selective area growth of monolithically integrated 1550-nm distributed feedback and electroabsorption modulator for 10 Gb/s operation.

Mark Skuse was born in Woodbridge, Suffolk, U.K., in 1965.

In 1992, he was at Agilent Technologies (formerly Hewlett Packard and BT&D), where he was engaged in epitaxy working on metal–organic vapor-phase epitaxy reactors and characterization of various semiconductor devices. Since 2007, he has been at CIP Technologies, Martlesham Heath, Ipswich, U.K, where he has been involved in device fabrication offering technical support processing various devices, including photodiodes and SOAs.

Richard J. Firth was born in Stoughton, MA. He received a higher national certificate in mechanical and manufacturing engineering, in 1998 from Suffolk College of Higher and Further Education, Ipswich, U.K.

In 1994, he was at Agilent Technologies, U.K. (formerly Hewlett Packard), where he was working on various optoelectronic device fabrication and process development. In 2000, he was at Corning Research Center, U.K. (formerly BT Research Laboratories), where he was engaged in research on electroabsorption modulator fabrication and design. Since 2003, he has been at CIP Technologies, Martlesham Heath, Ipswich, U.K. His current research interests include engineering and design support for semiconductor and planar-silica fabrication, photonic integration, and optical thin-film technologies.